Three-actuator deformable water-cooled mirror

Anthony Fuschetto
The Perkin-Elmer Corporation
Electro-Optical Division
Danbury, Connecticut 06810

Abstract. A new method for dynamically deforming a thin mirror to correct the phase aberration function for defocus and astigmatism is presented. Three piezoelectric-type actuators, attached to the back edges and parallel to the front surface of the mirror, induce edge moments that bend the mirror to its desired shape for correction of the aberrated wavefront. A three-actuator deformable water-cooled mirror breadboard has been designed and built. Major features, design constraints, and performance expectations of the deformable mirror design are described.

Keywords: active optics; deformable mirrors; wavefront corrections; NASTRAN analysis.

Optical Engineering 20(2), 310-315 (March/April 1981).

CONTENTS

1. Introduction
2. Cylinder actuation
3. Major features/components
4. Design criteria
   4.1. Wavefront corrections
   4.2. Surface figure error
   4.3. Cooling
   4.4. Hydraulic and thermal distortions
   4.5. System bandwidth
   4.6. Surface error intensity weighted
5. NASTRAN analysis
6. Summary of deformable mirror design analysis
7. Conclusion
8. Acknowledgments

1. INTRODUCTION

The conventional method in deforming a thin mirror for aberration control has been to use a large number of actuators operating normal to the backface of the mirror. A typical arrangement, shown in Fig. 1, is to mount the actuators on about 1-inch centers in some established grid pattern, usually triangular or square. For the deformable mirror under consideration, using the conventional criteria for aberration corrections would require at least 19 actuators.

This paper describes the development of a simple novel deformable mirror which provides the required mode control for focus and astigmatism with only three actuators. The desired contours for defocus, P_4, and astigmatism, P_5 and P_6, are combinations of Zernike polynomials (Figs. 2 through 4) where

$P_4 = A_4 (2r^2 - 1)$ which is corrected by changing the radius of curvature of the mirror,

$P_5 = A_5 r_2 \cos 2\theta$ which is corrected by a cylindrical contour at 0°,

$P_6 = A_6 r^2 \sin 2\theta$ which is corrected by a cylindrical contour at 45°.

If you consider a mirror working at normal incidence, the phase aberration function for focus and astigmatism is equivalent to three cylinders at 0, 90, and 45 degrees with respect to each other. As shown in Fig. 5, by mounting three actuators parallel to the mirror face, rather than the conventional normal to mirror face multimounting, it is possible to bend the mirror into a cylindrical shape with a single actuator.

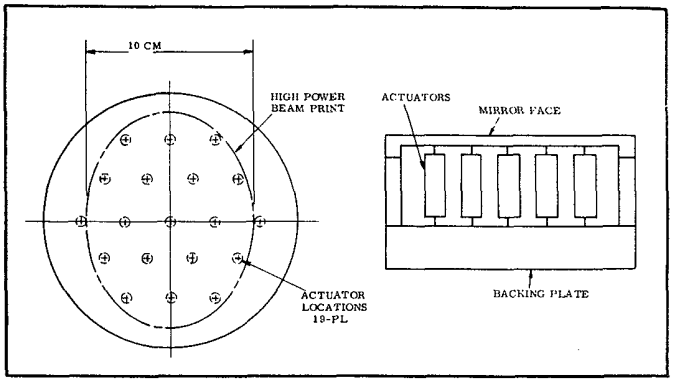

Fig. 1. Conventional multimounting deformable mirror.

2. CYLINDER ACTUATION

As illustrated in Fig. 5, each actuator, which consists of two in-line piezoelectric stacks, is attached to the back of the mirror near its outside edges. Axial motions of the actuator provide equal and opposite bending moments about the edges of the mirror, resulting in an almost cylindrically shaped curve of the mirror surface. Since the actuators are eccentric with respect to the neutral axis of the mirror, in addition to the moments at the mirror edge there are transverse forces acting in tension (push mode) or compression (pull mode). These transverse forces produce negligible deflections since the mirror is a short beam, and, as a result, the bending moments may be assumed to be constant along the length of the beam. The equation for bending of the mirror is therefore essentially the same as a cantilever bent by a couple Pe applied at the end , that is

$$R = \frac{EI}{M}, \qquad (1)$$

where R is the radius of curvature, E is modulus of elasticity, I is the moment of inertia, and M is end moment.

If E, I, and M are constant, the radius R is a constant, and the deflection surface is a true cylinder. Since the mirror is round, the moment of inertia varies from edge to center; however, this variation causes the deflection surface to vary by only 7% maximum from a

Invited Paper 5060 received April 28, 1980; revised manuscript received June 18, 1980; accepted for publication June 24, 1980; received by Managing Editor June 30, 1980. This paper is a revision of Paper 179-03 which was presented at the SPIE seminar on Adaptive Optical Components, April 19-20, 1979, Washington, D. C. The paper presented there appears (unrefereed) in SPIE Proceedings Vol. 179.

cylinder at the outer edge of the beam print. The deflection equation of the mirror surface, taking into account the variable moment of inertia, is

$$y = \frac{6(Pe)(1-w^2)}{Eh^3}\left[x \sin^{-1}\left(\frac{x}{r}\right) + \sqrt{R^2-x^2} - R\right], \quad (2)$$

where y is the sag, P is the actuator force, e is eccentricity, w is Poisson's ratio, x is the distance from the center, and R is the radius of the mirror. The mirror slope equation is

$$\Theta = \frac{6(Pe)(1-w^2)}{Eh^3} \sin^{-1}\left(\frac{x}{r}\right). \quad (3)$$

The actuator displacement (δ_h) equation is

$$\delta_h = e\Theta. \quad (4)$$

The above equations, which were developed by the author to approximate the mirror deflections, actuator forces, and displacements for the intitial mirror design, are idealized since they do not consider the interaction and stiffness of the actuators in bending of the mirror. To predict more accurately the actual mirror characteristics, an optimized detailed NASTRAN model was performed, the results of which are discussed in a later section.

3. MAJOR FEATURES/COMPONENTS

The three-actuator deformable mirror configuration is shown in Fig. 6. Basically, the deformable mirror assembly consists of the H_2O cooled mirror substrate, the piezoceramic actuator assembly, the position pickoffs, and the base plate.

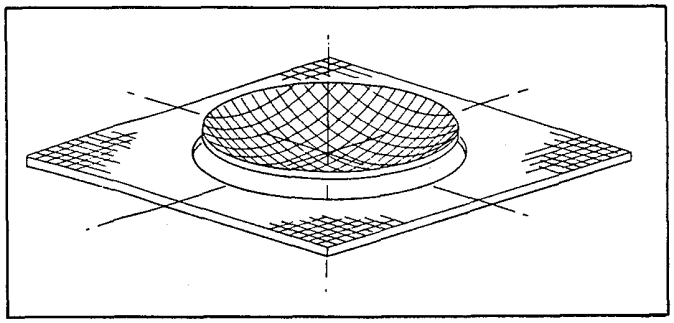

Fig. 2. P_4 focus ($2r^2 - 1$).

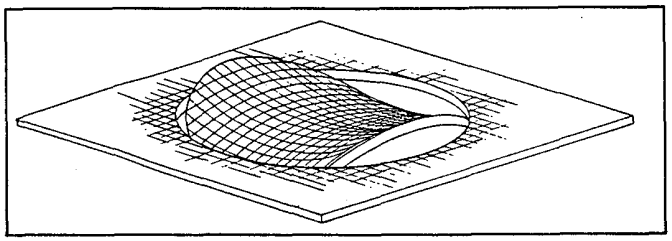

Fig. 3. P_5 zero-degree third-order astigmatism.

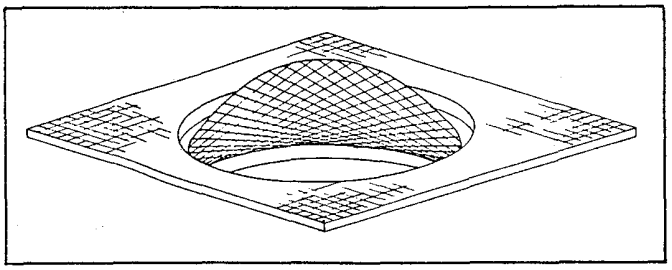

Fig. 4. P_6 45-degree third-order astigmatism.

The 6 inch diameter by 5/16 inch thick deformable mirror substrate is an all molybdenum, brazed assembly consisting of three individually machined sections: the faceplate/heat exchanger, the manifold plate, and the backing plate.

The piezoceramic actuator assembly consists of three actuators. Each actuator, made up of two in-line stacks with 44 disks per stack, is joined at the center to a floating beryllium block. The ends of the actuators are attached to the back of the mirror. Single blade flexural members at each end of the stacks are used to take up in-plane misalignment, and to act as hinges so as to minimize bending restraint of the mirror.

Gulton Industries G1512 piezoceramic material was used as a basis for sizing the actuators. With this material a total swing of ±30 V/mil can be obtained if a dc bias of 15 V/mil is applied in the poling direction to produce a +45 V/mil positive and 15 V/mil negative swing. The charge coefficient (d_{33}) for the G1512 material, which is 500×10^{-12} m/V, provides a stack stroke capability of $\pm9.44\times10^{-4}$ inch using a ±1000 V supply.

The six position pickoffs, which are Kaman Sciences (KD2810-1μ) eddy current type sensors, are located between the mirror and base plate and sense the back surface of the mirror at the footprint of the high-power beam. These position sensors provide for cage/closed loop control of the mirror. The resolution and repeatability of these sensors over the range of mirror displacements are better than 0.1 μm.

The beryllium base plate acts as the reference surface and support member for the deformable mirror via the fixed center post and the position pickoffs.

4. DESIGN CRITERIA

4.1. Wavefront corrections

The main criteria for the deformable mirror design are based on achieving, as a minimum, peak-to-peak wavefront corrections of ±1-wave defocus and ±1/2-wave astigmatism, acting separately or

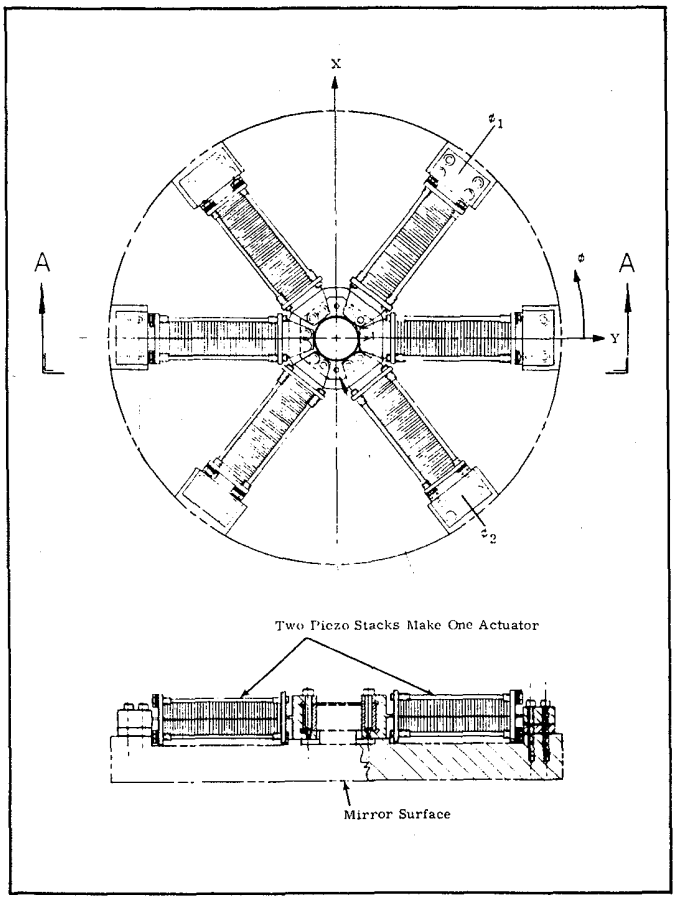

Fig. 5. Three-actuator deformable mirror.

simultaneously at 9.27 μm. These wavefront corrections are made by bending the mirror about the x, y, and ϕ (37.91°) axes with three actuators as discussed in the previous sections. The reason for orienting the ϕ-axis at 37.91° and not 45° is because the deformable mirror is working at an angle with respect to the incident beam normal in the actual system. Projecting the 45° astigmatism axis in the plane of the beam onto the elliptical beam print results in a rotation of the cylinder axis from 45° to 37.91°.

4.2. Surface figure error

The OPD rms surface tolerance conformance is within 0.12 μm, with peak wavefront corrections.

4.3. Cooling

The system is H_2O cooled, with flow rate of 11 gal/min.

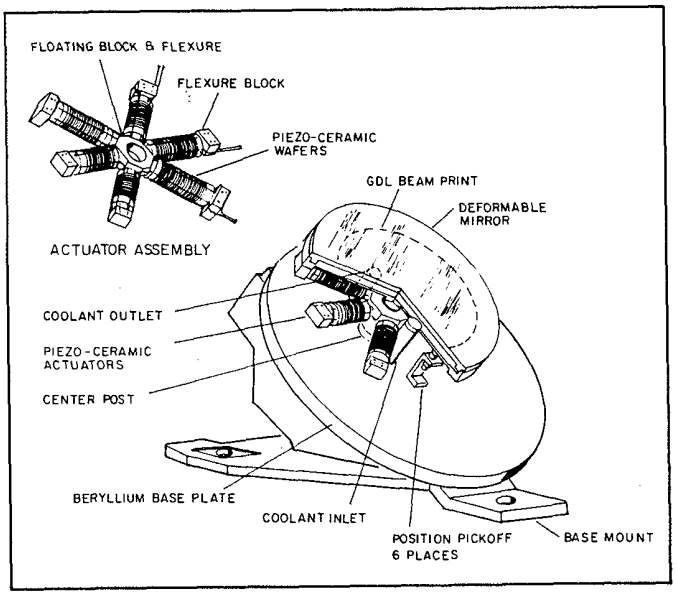

Fig. 6. Three-actuator deformable mirror assembly.

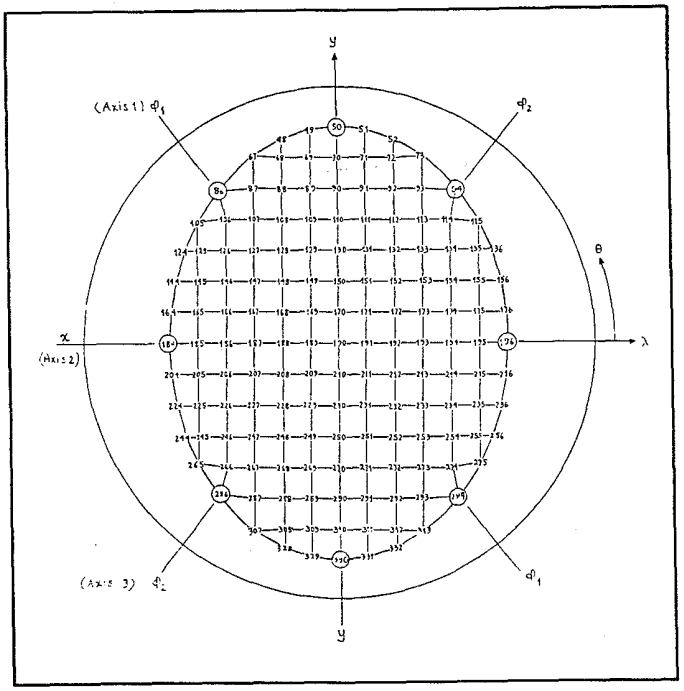

Fig. 7. NASTRAN model, grid points covering the region of the aperture.

4.4. Hydraulic and thermal distortions

Hydraulic and thermal distortions are less than 15 micro-inches. Out of plane (sag) thermal distortion is removed by actuators.

4.5. System bandwidth

System bandwidth is at least 100 Hz, with no mirror structural resonances less than 750 Hz.

4.6. Surface error intensity weighted

For optimization, the calculated OPD rms surface error was intensity weighted. The intensity weighted surface error is the product of the intensities of the laser beam on the mirror surface and the phase OPD on the corresponding point on the surface, divided by the beam's average intensity. Intensity weighting of the mirror OPD has the effect of weighting more heavily the areas of the mirror surface where the laser beam intensity is high and less heavily those where it is low.

5. NASTRAN ANALYSIS

The calculated results for figure error are based on a detailed NASTRAN analysis that accurately modeled the configuration of the

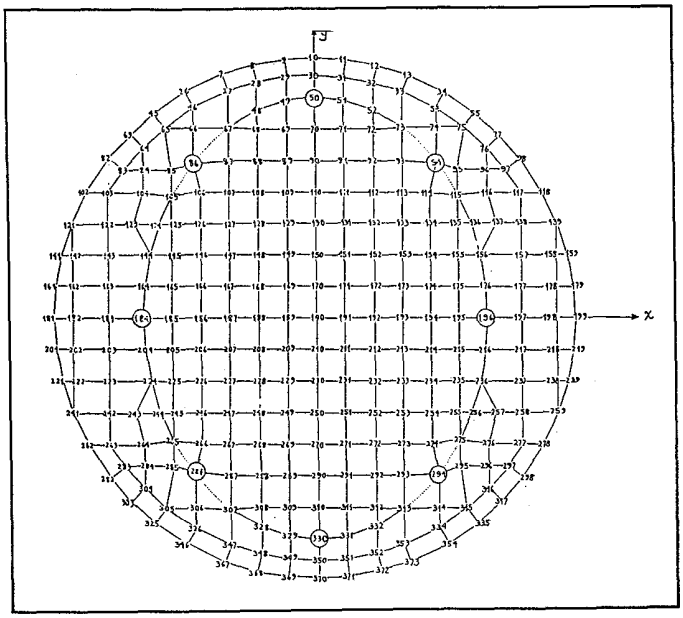

Fig. 8. NASTRAN model, grid points covering the region of the entire mirror.

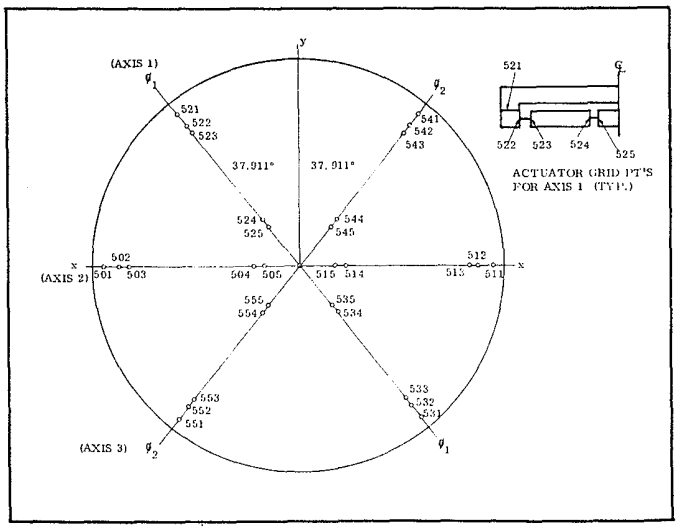

Fig. 9. NASTRAN model, grid points covering the region of the actuators.

deformable mirror assembly. Included in the model were exact detail properties of the mirror, flexure blocks, piezoceramic actuators, and bonding agent, and the floating block/flexures. Figures 7, 8, and 9 show the NASTRAN model.

The NASTRAN analysis provided the influence coefficients for grid point displacement and element stresses for unit actuation force. Using the influence coefficients, the displacements at the grid points were established. The forces were determined so as to mathematically minimize the rms OPD error. Knowing the forces and influence coefficients of the model, the deflections at all grid points were calculated. Defocus, astigmatism, and their combination, and thermal distortions were analyzed for correction and residual errors. The analytical results, as summarized in the following section, show that the surface figure met the design goals.

6. SUMMARY OF DEFORMABLE MIRROR DESIGN ANALYSIS

A summary of the deformable mirror performance as a result of the detailed NASTRAN analysis is provided in Tables I through IV and Figs. 10 through 15 in the following order:

- Table 1. Surface Conformance
- Table 2. Thermal/Hydraulic Distortion Errors
- Table 3. Actuator Displacement Requirements
- Table 4. Mirror Resonances/Modes
- Figures 10–15. OPD Contour Plots for Defocus/Astigmatism, Combined Defocus and Astigmatism, and Thermal Distortion Using Intensity Weight Factors.

TABLE I. Surface Conformance

Case No.	Type of Abberation	Zernike Polynomial Expression	Wavelength (μm)	Required Wavefront Corrections (Waves)	Allowed OPD rms Tolerance (μm)	Calculated OPD rms Error, Intensity Weighted (μm)
1	Defocus P_4	$A_4 (2r^2 - 1)$	9.27	± 1	0.187	0.081
2	Astigmatism P_5	$A_5 r_2 \cos 2\theta$	9.27	$\pm 1/2$	0.187	0.063
3	Astigmatism P_6	$A_6 r_2 \sin 2\theta$	9.27	$\pm 1/2$	0.187	0.049
4	P_4 + P_5	$A_4 (2r^2 - 1)$ + $A_5 r_2 \cos 2\theta$	9.27	± 1 + $\pm 1/2$	0.187	0.123
5	P_4 + P_6	$A_4 (2r^2 - 1)$ + $A_6 r_2 \sin 2\theta$	9.27	± 1 + $\pm 1/2$	0.187	0.095

Notes
1. Analysis is based on 10-cm beam size.
2. Surface error OPD_{rms} is proportional to wavefront correction.
3. Surface error OPE_{rms} is minimized as a result of minimizing the mean square error.

TABLE II. Thermal/Hydraulic Distortion Errors

Uncorrected Thermal Distortions

1. Thermal growth:

Faceplate	0.061 μm
Channel	0.038 μm
Substrate	0.188 μm
Total	0.287 μm

2. Thermal bowing and Poisson's effect:

Ends of major axis	Point 50	1.905 μm
	Point 330	1.956 μm
Ends of minor axis	Point 184	1.346 μm
	Point 196	1.498 μm

Corrected Thermal Distortions

1. Decomposition into Zernike Polynomials
2. From contour plots peak OPD error in the region of the beam does not exceed 0.4 μm, except one spot 0.445 μm.

Hydraulic Distortion Errors:

1. Plate Deflection	- 0.006 μm
2. Fin deflection	- 0.022 μm
Total	- 0.028 μm

50% of this error will be removed by polishing mirror at average operating pressure.

TABLE 3. Actuator Displacement Requirements

Actuator Displacements Required for Peak Wavefront Corrections

Type of Aberration	Actuator Displacement, Inches (Intensity Weighted)		
	Axis 1	Axis 2	Axis 3
P_4	0.000351	0.000257	0.000352
P_5	−0.000087	0.000272	−0.000086
P_6	0.000175	−0.000547	−0.000173
$P_4 + P_5$	0.000264	0.000529	0.000265
$P_4 + P_6$	0.000526	0.000257	0.000178

Actuator Displacements Required for Correction of Thermal Errors
(Cyle IV Intensity Weighted)

Axis 1:	0.000115 Inch
Axis 2:	0.000066 Inch
Axis 3:	0.000114 Inch

Total Maximum Actuator Displacements Required

Axis 1:	0.000641 Inch
Axis 2:	0.000595 Inch
Axis 3:	0.000466 Inch

TABLE IV. Mirror Resonances/Modes

Mode No.	Frequency (Hertz)	Mode Description
1.	163	• Dish-shaped deflection of floating centerpiece • Very loose coupling mirror surface—less than 0.6%
2.	355	• S-shaped deflection of actuators due to flexures • For the mirror it is mostly a tilt about y-axis
3.	359	• Rotation about z-axis • Very loose coupling to mirror surface—less than ±0.3%
4.	380	• Similar to mode 2 except that now it is a tilt about x-axis
5.	533	• Floating block rotation about y-axis • Causes slight mirror tilt about y-axis
6.	581	• Floating block rotation about x-axis • Causes slight mirror rotation about x-axis
7.	1,056	• Dish-shaped deflection of mirror

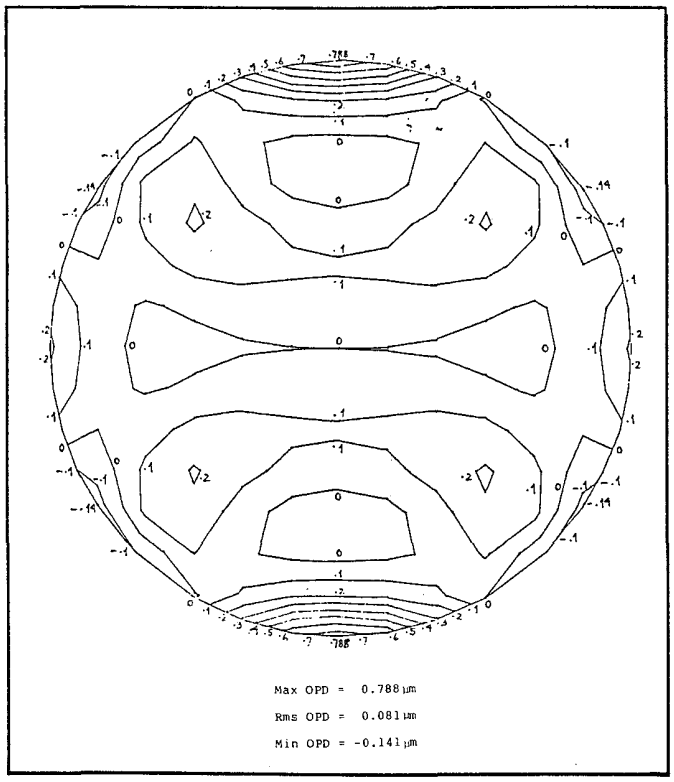

Fig. 10. P_4 defocus OPD theoretical residual error contour plot in μm for $1\lambda(\lambda = 9.27\,\mu m)$ wavefront correction (optimization using intensity weight factors).

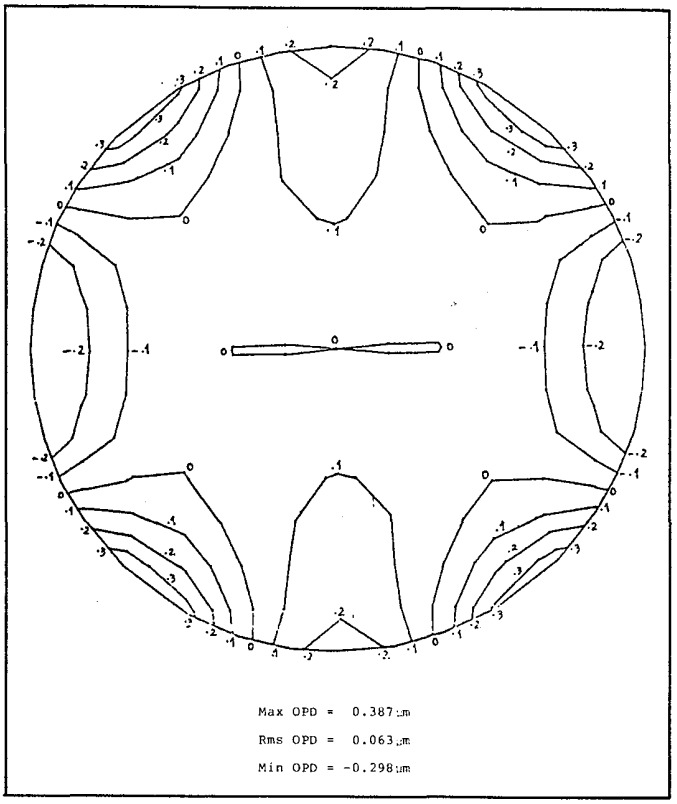

Fig. 11. P_5 (0°) astigmatism OPD theoretical residual error contour plot in μm for $1/2\lambda(\lambda = 9.27\,\mu m)$ wavefront correction (optimization using intensity weight factors).

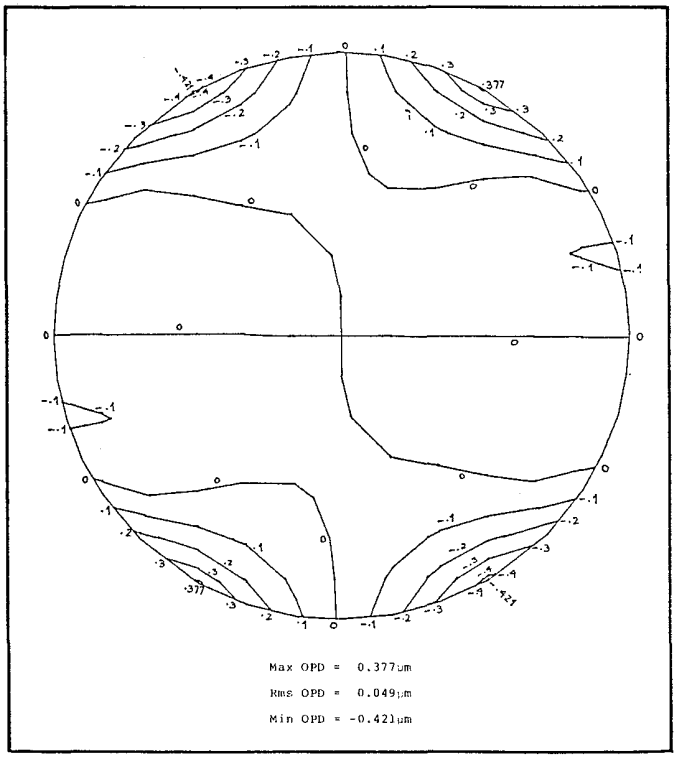

Fig. 12. P_6 (45°) astigmatism OPD theoretical residual error contour plot in μm for $1/2\lambda(\lambda = 9.27\,\mu m)$ wavefront correction (optimization using intensity weight factors).

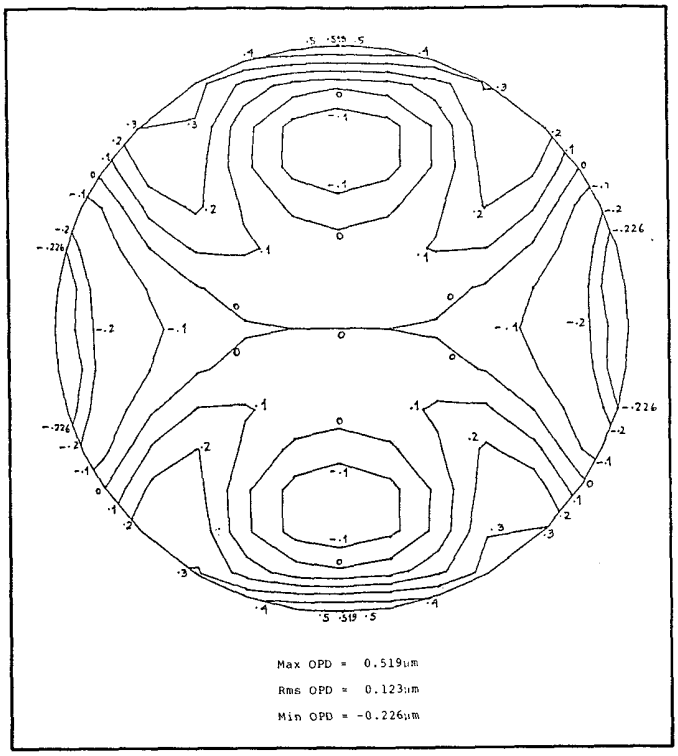

Fig. 13. P_4 and P_5 combined defocus and 0° astigmatism OPD theoretical residual error contour plot in μm for 1 λ defocus and 1/2 λ astigmatism (λ = 9.27 μm) wavefront correction (optimization using intensity weight factors).

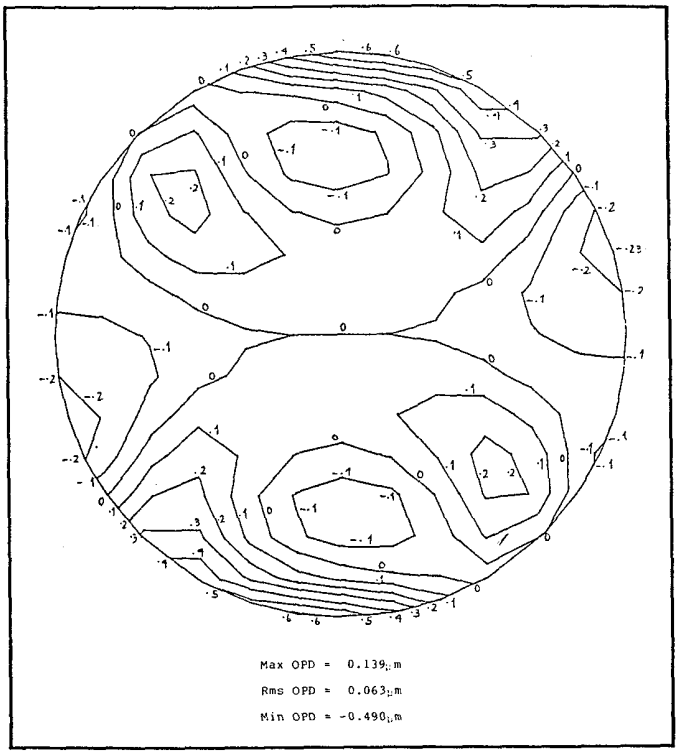

Fig. 15. Thermal distortion OPD theoretical residual error contour plot in μm after correcting for a specified thermal loading (optimization using intensity weight factors).

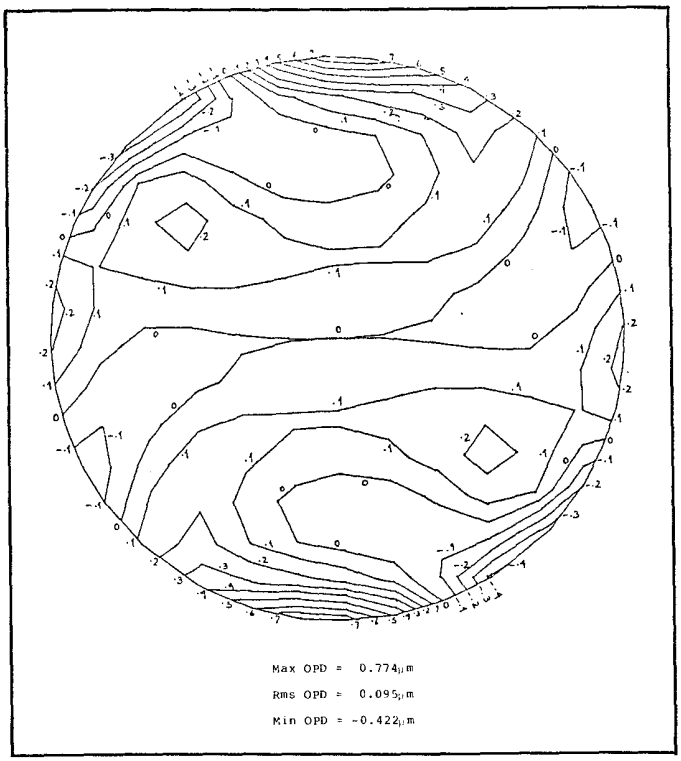

Fig. 14. P_4 and P_6 combined defocus and 45° astigmatism OPD theoretical residual error contour plot in μm for 1 λ defocus and 1/2 λ astigmatism (λ = 9.27 μm) wavefront correction (optimization using intensity weight factors).

7. CONCLUSION

A new method for actively deforming a thin mirror by using only three actuators to perform aberrated wavefront corrections of focus and astigmatism has been described. The mirror performance results from the detailed analysis are quite favorable. Perkin-Elmer is in the process of assembly of the three-actuator deformable mirror breadboard with the hope of conducting a very sophisticated test program in the next several months to verify actual performance.*

8. ACKNOWLEDGMENTS

The author wishes to thank Norbert Schnog of Perkin-Elmer for his inspiration and help in the development of the three-actuator deformable mirror concept. Additional thanks are extended to Pravin Mehta of Perkin-Elmer for his significant contribution of OPD minimization and NASTRAN analysis.

The work leading to this paper was performed under Contract No. 77-C-0062 with the Air Force Weapons Laboratory.

* Since this paper was presented at the SPIE seminar on Adaptive Optical Components, April 19-20, 1979, Washington D.C., Perkin-Elmer has built and functionally tested two "Three Actuator Deformable Mirror" assemblies, a breadboard, and flight unit. Both mirrors exhibited favorable performance and were delivered under contract to the Air Force Weapons Laboratory.